ISSN 2070-0482, Mathematical Models and Computer Simulations, 2013, Vol. 5, No. 4, pp. 360–370. © Pleiades Publishing, Ltd., 2013.
Original Russian Text © U.S. Abdibekov, B.T. Zhumagulov, D.B. Zhakebayev, K.Zh. Zhubat, 2013, published in Matematicheskoe Modelirovanie, 2013, Vol. 25, No. 1, pp. 18–32.

Simulation of Isotropic Turbulence Degeneration Based on the Large-Eddy Method

U. S. Abdibekov, B. T. Zhumagulov, D. B. Zhakebayev, and K. Zh. Zhubat

Al-Farabi Kazakh National University, Almaty, Kazakhstan

e-mail: uali1@mail.ru, daurjaz@mail.ru

Received July 26, 2011

Abstract—In this paper, the simulation of isotropic turbulence degeneration is studied. The turbulent process is modeled based on filtered three-dimensional unsteady Navier–Stokes equations. For the closure of the main equations, a viscous model of turbulence is used. The problem is solved numerically, i.e., in solving the equation of motion the modified method of fractional steps using compact schemes is employed and the equation for pressure is solved by the Fourier method in combination with matrix factorization. Temporal variations in the kinetic energy of turbulence and changes in the micro scale of turbulence and longitudinal-transverse correlation functions have been obtained. Longitudinal and transverse one-dimensional spectra have been found.

Keywords: isotropic turbulence, Navier–Stokes equation, longitudinal-transverse correlation functions, micro scale of turbulence

DOI: 10.1134/S2070048213040029

1. INTRODUCTION

In studies of the homogenous turbulence degeneration experimentally, there is always a boundary of the measured space or the finite volume. Numerous experiments on the degeneration of grid-induced turbulence in a wind tunnel failed to provide the complete picture of degeneration because of the limited length of the test section. The known analytical methods are limited in describing the degeneration process because they neglect the influence of the pressure and other forces. Thus, today the numerical simulation is the only method for modeling the turbulence degeneration.

The investigation into the degeneration of homogeneous isotropic turbulence is usually based on spectral equations and equations of correlation functions, whose closure requires that certain correlation functions should be determined. This circumstance renders this approach inefficient because it is impossible to obtain the spectra for a large time interval and at the moment of the main dissipation [1, 2].

In this work, we make an attempt at solving this problem by using the large-eddy method. The idea is to impose in the phase space the initial condition for the field of velocities that satisfies the condition for continuity. In doing this, the main spectral equation is not solved and the set initial condition is transferred from the phase space into the physical space using the Fourier transform. The obtained field of velocities
1 is used as the initial condition for the filtered Navier–Stokes equation. Then, the nonstationary three-dimensional Navier–Stokes equation is solved to simulate the degeneration of the isotropic turbulence.

2. PROBLEM STATEMENT

The isotropic medium in turbulence undergoes a very rapid homogeneous deformation; then, all the characteristic sizes and any averaged characteristics of turbulence are constant but variable in time. In order to determine turbulent characteristics, it is necessary to numerically model the time variation change in all the parameters and the degeneration of the isotropic turbulence at different Reynolds numbers.

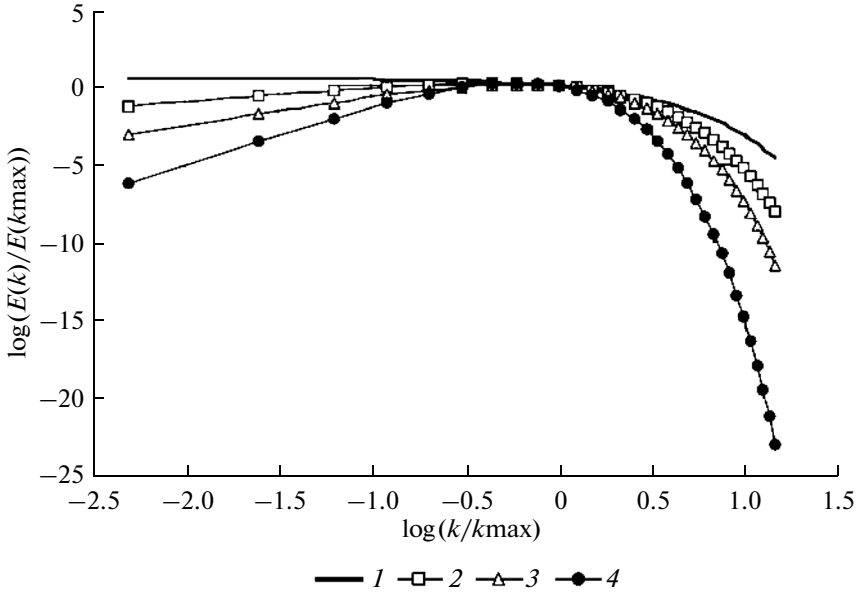

Fig. 1. Energy of the initial level of turbulence based on the fixed wave number $k_{\max} = 20$ and variation parameter m: (1) $m = 2$; (2) $m = 4$; (3) $m = 6$; (4) $m = 8$.

1 The numerical modeling of the problem is based on the solution of nonstationary filtered Navier–Stokes equations with the continuity equation in the Cartesian coordinate system

$$\begin{cases} \dfrac{\partial \overline{u}_i}{\partial t} + \dfrac{\partial}{\partial x_j}\left(\overline{u}_i \overline{u}_j\right) = -\dfrac{1}{\rho}\dfrac{\partial \overline{p}}{\partial x_i} + \dfrac{1}{\mathrm{Re}}\dfrac{\partial^2 \overline{u}_i}{\partial x_j \partial x_j} - \dfrac{\partial \tau_{ij}}{\partial x_j}, \\ \dfrac{\partial \overline{u}_i}{\partial x_i} = 0, \\ \tau_{ij} = \overline{u_i u_j} - \overline{u}_i \overline{u}_j, \end{cases} \tag{1}$$

where $\overline{u}_i$ are velocity components, $\overline{p}$ is the pressure, t is the time, ν is the kinematic coefficient of viscosity, and $\tau_{i,j}$ is the subgrid tensor responsible for small scale structures to be simulated, i, j—1, 2, 3.

For modeling f the subgrid tensor a viscosity model is used and is represented as

$$\tau_{ij} - \frac{\delta_{ij}}{3}\tau_{kk} = -2\nu_T \overline{S}_{ij},$$

where $\nu_T = C_S \Delta^2 \left(2\overline{S}_{ij}\overline{S}_{ij}\right)^{1/2}$ is the turbulence viscosity, C_S is the empirical coefficient, $\Delta = \left(\Delta_i \Delta_j \Delta_k\right)^{1/3}$ is the width of the grid filter, and $\overline{S}_{ij} = \dfrac{1}{2}\left(\dfrac{\partial \overline{u}_i}{\partial x_j} + \dfrac{\partial \overline{u}_j}{\partial x_i}\right)$ is the value of the tensor of deformation of velocities [3, 4].

Boundary conditions are taken as periodic in all directions.The initial values for each component are assigned as functions dependent on wave numbers in the phase space

$$\hat{u}_1(k_1, 0) = k_1^{\frac{m-2}{2}} e^{-\frac{m}{4}\left(\frac{k_1}{k_{\max}}\right)}, \quad \hat{u}_2(k_2, 0) = k_2^{\frac{m-2}{2}} e^{-\frac{m}{4}\left(\frac{k_2}{k_{\max}}\right)}, \quad \hat{u}_2(k_2, 0) = k_3^{\frac{m-2}{2}} e^{-\frac{m}{4}\left(\frac{k_3}{k_{\max}}\right)},$$

where $\hat{u}_1$ is the one-dimensional longitudinal spectrum spectrum, while $\hat{u}_2$ and $\hat{u}_3$ are the one-dimensional lateral spectrum.

For this problem a variation parameter m and the wave number $k_{\max}$, which determine the kind of turbulence, are chosen. In Fig. 1, at $k_{\max} = 20$ parameter, m varies. In modeling the isotropic turbulence, it is possible to take parameters $k_{\max} = 20$ and $m = 4$, corresponding to the experimental data [5].

The assigned initial condition is transferred from the phase space into the physical space using the Fourier transform.

3. NUMERICAL METHOD

In solving the Navier–Stokes equation (1), use is made of a scheme split by physical parameters that consists of three stages. At the first stage, the Navier–Stokes equation is solved, without taking pressure into account. For approximation of the convective and diffusion terms of the equation a compact scheme of a higher order of accuracy [6] is used.

The intermediate field of velocity is found by the fractional step method [7] using the sweep method. The fractional step method is employed for the horizontal component of velocity u_1 at the grid point $(i+1/2, j, k)$. In order to use compact schemes, the fractional step method is modified. At the first stage

$$\begin{cases} \dfrac{\overline{u}^{*}_{1i+1/2,j,k} - \overline{u}^{n}_{1i+1/2,j,k}}{\tau} = \left(\dfrac{1}{2}\Lambda_{1k}\overline{u}^{*}_{1i+1/2,j,k} + \dfrac{1}{2}\Lambda_{1k}\overline{u}^{n}_{1i+1/2,j,k}\right) + \Lambda_{2}\overline{u}^{n}_{1i+1/2,j,k} + \Lambda_{3}\overline{u}^{n}_{1i+1/2,j,k}, \\ \dfrac{\overline{u}^{n+1/3}_{1i+1/2,j,k} - \overline{u}^{*}_{1i+1/2,j,k}}{\tau} = \left(\dfrac{1}{2}\Lambda_{1d}\overline{u}^{n+1/3}_{1i+1/2,j,k} + \dfrac{1}{2}\Lambda_{1d}\overline{u}^{*}_{1i+1/2,j,k}\right), \end{cases} \tag{2}$$

where

$$\Lambda_{1k}\overline{u}_{1i+1/2,j,k} = -\overline{u}_1 \frac{\partial}{\partial x_1}(\overline{u}_1)\Big|_{i+1/2,j,k}; \quad \Lambda_{1d}\overline{u}_{1i+1/2,j,k} = \frac{1}{\mathrm{Re}}\frac{\partial}{\partial x_1}\left(\frac{\partial \overline{u}_1}{\partial x_1}\right)\Bigg|_{i+1/2,j,k}.$$

The second stage is given by

$$\begin{cases} \dfrac{\overline{u}^{*}_{1i+1/2,j,k} - \overline{u}^{n+1/3}_{1i+1/2,j,k}}{\tau} = \left(\dfrac{1}{2}\Lambda_{2k}\overline{u}^{*}_{1i+1/2,j,k} + \dfrac{1}{2}\Lambda_{2k}\overline{u}^{n}_{1i+1/2,j,k}\right) - \Lambda_{2}\overline{u}^{n}_{1i+1/2,j,k}, \\ \dfrac{\overline{u}^{n+2/3}_{1i+1/2,j,k} - \overline{u}^{*}_{1i+1/2,j,k}}{\tau} = \left(\dfrac{1}{2}\Lambda_{2d}\overline{u}^{n+2/3}_{1i+1/2,j,k} + \dfrac{1}{2}\Lambda_{2d}\overline{u}^{*}_{1i+1/2,j,k}\right), \end{cases} \tag{3}$$

where

$$\Lambda_{2k}\overline{u}_{1i+1/2,j,k} = -\overline{u}_2 \frac{\partial}{\partial x_2}(\overline{u}_1)\Big|_{i+1/2,j,k}; \quad \Lambda_{2d}\overline{u}_{1i+1/2,j,k} = \frac{1}{\mathrm{Re}}\frac{\partial}{\partial x_2}\left(\frac{\partial \overline{u}_1}{\partial x_2}\right)\Bigg|_{i+1/2,j,k}.$$

The third stage is given by

$$\begin{cases} \dfrac{\overline{u}^{*}_{1i+1/2,j,k} - \overline{u}^{n+2/3}_{1i+1/2,j,k}}{\tau} = \left(\dfrac{1}{2}\Lambda_{3k}\overline{u}^{*}_{1i+1/2,j,k} + \dfrac{1}{2}\Lambda_{3k}\overline{u}^{n}_{1i+1/2,j,k}\right) - \Lambda_{3}\overline{u}^{n}_{1i+1/2,j,k}, \\ \dfrac{\overline{u}^{n+1}_{1i+1/2,j,k} - \overline{u}^{*}_{1i+1/2,j,k}}{\tau} = \left(\dfrac{1}{2}\Lambda_{3d}\overline{u}^{n+1}_{1i+1/2,j,k} + \dfrac{1}{2}\Lambda_{3d}\overline{u}^{*}_{1i+1/2,j,k}\right), \end{cases} \tag{4}$$

where

$$\Lambda_{3k}\overline{u}_{1i+1/2,j,k} = -\overline{u}_3 \frac{\partial}{\partial x_3}(\overline{u}_1)\Big|_{i+1/2,j,k}; \quad \Lambda_{3d}\overline{u}_{1i+1/2,j,k} = \frac{1}{\mathrm{Re}}\frac{\partial}{\partial x_3}\left(\frac{\partial \overline{u}_1}{\partial x_3}\right)\Bigg|_{i+1/2,j,k}.$$

By using the scheme with upwind differences [8] and the compact scheme, we obtain a scheme with a high-order accuracy. The compact scheme for convective terms of equations with $A = \overline{u}_1 > 0$ has the following form:

$$\Lambda_{1k}\overline{u}_{1i+1/2,j,k} = -\overline{u}_1 \frac{\partial}{\partial x_1}(\overline{u}_1). \tag{5}$$

The traditional formulation of the derivative (5) approximation has the form

$$\Lambda_{1k}\overline{u}_{1i,j,k} = \begin{cases} -A\dfrac{\overline{u}_{1i,j,k} - \overline{u}_{1i-1/2,j,k}}{\Delta x}, & A > 0, \\ -A\dfrac{\overline{u}_{1i+1/2,j,k} - \overline{u}_{1i,j,k}}{\Delta x}, & A < 0. \end{cases}$$

We introduce denotation

$$f_{i,j,k} = -\frac{\overline{u}^n_{1i,j,k} - \overline{u}^n_{1i-1/2,j,k}}{\Delta x}, \quad A > 0. \tag{6}$$

The compact approximation of relationship (6) is as follows:

$$\alpha f_{i+1,j,k} + \beta f_{i,j,k} + \gamma f_{i-1,j,k} = -\frac{\overline{u}_{1i,j,k} - \overline{u}_{1i-1/2,j,k}}{\Delta x}. \tag{7}$$

We choose the indefinite coefficients so that the following relation should be satisfied:

$$\left|\left(\alpha f_{i+1,j,k} + \beta f_{i,j,k} + \gamma f_{i-1,j,k}\right) - \left(-\frac{\overline{u}_{1,j,k} - \overline{u}_{1i-1/2,j,k}}{\Delta x}\right)\right| = O\left(h^3\right). \tag{8}$$

To do this, we insert in (8) the Taylor-series expansions of functions $f(x, y, z)$ and $u(x, y, z)$ at the point $x = x_i$:

$$\begin{aligned} &\alpha\left(f_i + \Delta x f_x + \frac{\Delta x^2}{2} f_{xx} + \frac{\Delta x^3}{6} f_{xxx} + \frac{\Delta x^4}{24} f_{xxxx}\right) + \beta f_i \\ &+ \gamma\left(f_i - \Delta x f_x + \frac{\Delta x^2}{2} f_{xx} - \frac{\Delta x^3}{6} f_{xxx} + \frac{\Delta x^4}{24} f_{xxxx}\right) \\ &= -\frac{1}{\Delta x} u_{i,j,k} + \frac{1}{\Delta x}\left(u_i - \Delta x u_x + \frac{\Delta x^2}{2} u_{xx} - \frac{\Delta x^3}{6} u_{xxx} + \frac{\Delta x^4}{24} u_{xxxx}\right) + O\left(h^4\right). \end{aligned} \tag{9}$$

From (9) we obtain the system

$$\begin{cases} (\alpha + \beta + \gamma) = -1, \\ (\alpha - \gamma) = \frac{1}{2}, \\ (\alpha + \gamma) = -\frac{1}{3}. \end{cases} \tag{10}$$

By solving system (10), we determine

$$\alpha = \frac{1}{12}, \quad \beta = -\frac{2}{3}, \quad \gamma = -\frac{5}{12}. \tag{11}$$

The compact scheme for the diffusion terms of equations

$$\Lambda_{1d}\overline{u}_{1i+1/2,j,k} = \frac{1}{\mathrm{Re}}\frac{\partial}{\partial x_1}\left(\frac{\partial \overline{u}_1}{\partial x_1}\right). \tag{12}$$

The traditional presentation of the derivative (12) approximation is

$$\Lambda_{1d}\overline{u}_{1i,j,k} = \left(\frac{1}{\mathrm{Re}}\frac{\overline{u}_{1i+1/2,j,k} - 2\overline{u}_{1i,j,k} + \overline{u}_{1i-1/2,j,k}}{\Delta x^2}\right).$$

We introduce denotations

$$f_{i,j,k} = \frac{\overline{u}_{1i+1/2,j,k} - 2\overline{u}_{1i,j,k} + \overline{u}_{1i-1/2,j,k}}{\Delta x^2};$$

the compact approximation has the form

$$\alpha f_{i+1,j,k} + \beta f_{i,j,k} + \gamma f_{i-1,j,k} = \frac{\overline{u}_{1i+1/2,j,k} - 2\overline{u}_{1i,j,k} + \overline{u}_{1i-1/2,j,k}}{\Delta x^2}.$$

We choose the indefinite coefficients so that the relationship

$$\left|\left(\alpha f_{i+1,j,k} + \beta f_{i,j,k} + \gamma f_{i-1,j,k}\right) - \left(\frac{\overline{u}_{1i+1/2,j,k} - 2\overline{u}_{1i,j,k} + \overline{u}_{1i-1/2,j,k}}{\Delta x^2}\right)\right| = O\left(h^4\right)$$

is fulfilled for the Taylor series expansion

$$\begin{aligned}&\alpha\left(f_i+\Delta x f_x+\frac{\Delta x^2}{2}f_{xx}+\frac{\Delta x^3}{6}f_{xxx}+\frac{\Delta x^4}{24}f_{xxxx}\right)+\beta f_i\\&+\gamma\left(f_i-\Delta x f_x+\frac{\Delta x^2}{2}f_{xx}-\frac{\Delta x^3}{6}f_{xxx}+\frac{\Delta x^4}{24}f_{xxxx}\right)\\&=\frac{1}{\Delta x^2}\left(u_i+\Delta x u_x+\frac{\Delta x^2}{2}u_{xx}+\frac{\Delta x^3}{6}u_{xxx}+\frac{\Delta x^4}{24}u_{xxxx}\right)-\frac{2}{\Delta x^2}u_{i,j,k}\\&+\frac{1}{\Delta x^2}\left(u_i-\Delta x u_x+\frac{\Delta x^2}{2}u_{xx}-\frac{\Delta x^3}{6}u_{xxx}+\frac{\Delta x^4}{24}u_{xxxx}\right)+O\left(h^4\right).\end{aligned}\tag{13}$$

From (13) we obtain the system

$$\begin{cases}(\alpha+\beta+\gamma)=1,\\(\alpha-\gamma)=0,\\(\alpha+\gamma)=\dfrac{1}{6}.\end{cases}$$

From this we find

$$\alpha=\frac{1}{12},\quad \beta=\frac{5}{6},\quad \gamma=\frac{1}{12}.\tag{14}$$

We introduce the difference operator M_k: $M_k f_{i,j,k}=\alpha_k f_{i+1,j,k}+\beta_k f_{i,j,k}+\gamma_k f_{i-1,j,k}$, where the coefficients for the convective term, α_k, β_k, and γ_k, are found in (11). Then, (7) can be rewritten as $f_{i,j,k}=M_k^{-1}\left(-\dfrac{\overline{u}_{1i,j,k}-\overline{u}_{1i-1,j,k}}{\Delta x}\right)$. Thus, Eq. (5) will have the following form:

$$\Lambda_{1k}\overline{u}_{i,j,k}=M_k^{-1}A\left(-\frac{\overline{u}_{1i,j,k}-\overline{u}_{1i-1,j,k}}{\Delta x}\right).\tag{15}$$

We introduce the difference operator M_d: $M_d f_{i,j,k}=\alpha_d f_{i+1,j,k}+\beta_d f_{i,j,k}+\gamma_d f_{i-1,j,k}$, where α_k, β_k, and γ_d, i.e., the coefficients for the diffusion term, are determined in (14). Then (12), we will have the following form:

$$\Lambda_{1d}\overline{u}_{1i,j,k}=M_d^{-1}\left(\frac{1}{\mathrm{Re}}\frac{\overline{u}_{1i+1,j,k}-2\overline{u}_{1i,j,k}+\overline{u}_{1i-1,j,k}}{\Delta x^2}\right).\tag{16}$$

By substituting (15) and (16) in formulas (2), we obtain the final modified first stage

$$\begin{cases}\dfrac{\alpha_k\overline{u}^*_{1i+3/2,j,k}+\beta_k\overline{u}^*_{1i+1/2,j,k}+\gamma_k\overline{u}^*_{1i-1/2,j,k}\overline{u}}{\tau}-\dfrac{\alpha_k\overline{u}^n_{1i+3/2,j,k}+\beta_k\overline{u}^n_{1i+1/2,j,k}+\gamma_k\overline{u}^n_{1i-1/2,j,k}}{\tau}\\=\left(\dfrac{1}{2}\Lambda_{1k}\overline{u}^*_{1i+1/2,j,k}+\dfrac{1}{2}\Lambda_{1k}\overline{u}^n_{1i+1/2,j,k}\right)+\Lambda_2\overline{u}^n_{1i+1/2,j,k}+\Lambda_3\overline{u}^n_{1i+1/2,j,k},\\\dfrac{\alpha_d\overline{u}^{n+1/3}_{1i+3/2,j,k}+\beta_d\overline{u}^{n+1/3}_{1i+1/2,j,k}+\gamma_d\overline{u}^{n+1/3}_{1i-1/2,j,k}}{\tau}-\dfrac{\alpha_d\overline{u}^*_{1i+3/2,j,k}+\beta_d\overline{u}^*_{1i+1/2,j,k}+\gamma_d\overline{u}^*_{1i-1/2,j,k}}{\tau}\\=\left(\dfrac{1}{2}\Lambda_{1d}\overline{u}^{n+1/3}_{1i+1/2,j,k}+\dfrac{1}{2}\Lambda_{1d}\overline{u}^*_{1i+1/2,j,k}\right).\end{cases}\tag{17}$$

The difference solution (17) is effectively computed by means of a three-point sweep. For the second (3) and third (4) stages, this procedure is repeated. Other components of the velocity are found in the same way.

Thus, we obtain a compact approximation for the convective terms of the motion equations of the third, and for the diffusion terms of the fourth, order of accuracy.

At the second stage, the Poisson equation obtained from the continuity equation with account for the velocity field of the first stage is solved. For the solution of the three-dimensional Poisson equation an original algorithm has been developed, which is a spectral transformation into combinations with a matrix sweep [9–11]. The obtained pressure field is used at the third stage for the recount of the final velocity field.

4. CORRELATION AND SPECTRAL FUNCTIONS FOR OBTAINING THE CHARACTERISTICS OF ISOTROPIC TURBULENCE

Finding the turbulence characteristics in a physical space requires the volume averaging of different values. The averaged values will participate in the determination of turbulent characteristics [12, 13]. The value averaged over all the calculated domain that in this work is rectangular is calculated by the following formula:

$$\langle u_i \rangle = \frac{1}{(N_1+1)(N_2+1)(N_3+1)} \sum_{n=1}^{N_1+1} \sum_{m=1}^{N_2+1} \sum_{q=1}^{N_3+1} (u_i)_{n,m,q}.$$

Different coefficients of velocity correlation can be found as follows:

$$R_{i1}(r) = \frac{1}{2(N_1+1-r)(N_2+1)(N_3+1)\langle \overline{u}_i^2 \rangle} \left\{ \begin{array}{l} \sum\limits_{n=1}^{N_1+1-r} \sum\limits_{m=1}^{N_2+1} \sum\limits_{q=1}^{N_3+1} [\overline{u}_i(n,m,q)\overline{u}_i(n+r,m,q)] \\ + \sum\limits_{n=1+r}^{N_1+1} \sum\limits_{m=1}^{N_2+1} \sum\limits_{q=1}^{N_3+1} [\overline{u}_i(n,m,q)\overline{u}_i(n-r,m,q)] \end{array} \right\},$$

$$R_{i2}(r) = \frac{1}{2(N_1+1)(N_2+1-r)(N_3+1)\langle \overline{u}_i^2 \rangle} \left\{ \begin{array}{l} \sum\limits_{n=1}^{N_1+1} \sum\limits_{m=1}^{N_2+1-r} \sum\limits_{q=1}^{N_3+1} [\overline{u}_i(n,m,q)\overline{u}_i(n,m+r,q)] \\ + \sum\limits_{n=1}^{N_1+1} \sum\limits_{m=1+r}^{N_2+1} \sum\limits_{q=1}^{N_3+1} [\overline{u}_i(n,m,q)\overline{u}_i(n,m-r,q)] \end{array} \right\},$$

$$R_{i3}(r) = \frac{1}{2(N_1+1)(N_2+1)(N_3+1-r)\langle \overline{u}_i^2 \rangle} \left\{ \begin{array}{l} \sum\limits_{n=1}^{N_1+1} \sum\limits_{m=1}^{N_2+1} \sum\limits_{q=1}^{N_3+1-r} [\overline{u}_i(n,m,q)\overline{u}_i(n,m,q+r)] \\ + \sum\limits_{n=1}^{N_1+1} \sum\limits_{m=1}^{N_2+1} \sum\limits_{q=1+r}^{N_3+1} [\overline{u}_i(n,m,q)\overline{u}_i(n,m,q-r)] \end{array} \right\}.$$

The calculations were performed for $r = 1,2,..., N_i/2$. The formulas are presented as discrete analogs of continuous representations $R_{11}(\mathbf{r},t)$, $R_{22}(\mathbf{r},t)$, $R_{33}(\mathbf{r},t)$ of correlation coefficients.

For the isotropic turbulence, the longitudinal and transverse correlations are as follows [1, 14, 15]:

$$f(r,t) = \frac{R_{11}(r,t)}{R_{11}(0,t)}, \quad g_1(r,t) = \frac{R_{22}(r,t)}{R_{22}(0,t)}, \quad g_2(r,t) = \frac{R_{33}(r,t)}{R_{33}(0,t)}.$$

The micro scale of the length is determined by the relationship

$$\lambda_f = \left\{ \frac{2}{-f''(0)} \right\}^{1/2}, \quad \lambda_g = \left\{ \frac{2}{g''(0)} \right\}^{1/2},$$

and the integral scale is expressed as

$$\Lambda_f = \int_0^\infty f(r)dr, \quad \Lambda_g = \int_0^\infty g(r)dr.$$

The longitudinal and transversal spectra are as follows [1]:

$$F_1(k_1) = \frac{1}{2\pi} \int_{-\infty}^{\infty} e^{-ik_1 r} R_{11}(r)\,dr = \frac{1}{\pi} \int_0^\infty \cos(k_1 r) R_{11}(r)\,dr \geq 0,$$

$$F_2(k_2) = \frac{1}{2\pi} \int_{-\infty}^{\infty} e^{-ik_2 r} R_{22}(r)\,dr = \frac{1}{\pi} \int_0^\infty \cos(k_2 r) R_{22}(r)\,dr \geq 0,$$

the one-dimensional spectrum is

$$E_1(k) = F_1(k) + 2F_2(k),$$

and the three-dimensional spectrum is

$$E(k) = -k\frac{dE_1(k)}{dk}.$$

The energy dissipation is calculated by formula

$$\varepsilon(t) = 30\nu\frac{R_{11}(0,t)}{\lambda_f^2(t)}.$$

The turbulent kinetic energy is found in the following way:

$$E_{kin}(t) = \frac{1}{2}R_{ij}(0,t) = \int_0^\infty E_1(k)dk.$$

5. SIMULATION RESULTS

As a result of modeling, the characteristics of the isotropic turbulence are found. According to the semiempirical theory, the integral scale of turbulence grows with time. The results given in Fig. 2 illustrate the effect of viscosity on the internal structure of the turbulence. A change in the coefficient of the molecular viscosity leads to a proportional change in the integral scale. Figure 3 shows the change in the micro scale – λ^2 calculated at different Reynolds numbers: (1) Re = 5000; (2) Re = 10000 and (3) Re = 20000.

Figure 4 shows the change in the energy dissipation at different Reynolds numbers. The results shown in Fig. 5 illustrate the influence of viscosity on the degeneration of the kinetic energy of isotropic turbulence calculated at different Reynolds numbers: (1) Re = 5000; (2) Re = 10000 and (3) Re = 20000. As is seen in Figs. 4 and 5, at high Reynolds numbers, there are more energy containing eddies and, accordingly, the velocity of the energy dissipation is greater, which is natural in a physical experiment.

The correlation coefficients express the mean correlation relationship with respect to volume between the velocity components in different points. The greater the distances of the points between different velocity components the lower the coefficients of the correlation should be; i.e., they should be close to zero. Figure 6 shows the time variation of the longitudinal correlation function $f(r)$ calculated at Re = 20000. It is seen that with an increase in r, the values of the functions tend to zero. The pattern of the change in the correlations corresponds to the change in the correlation function given in [15, 16].

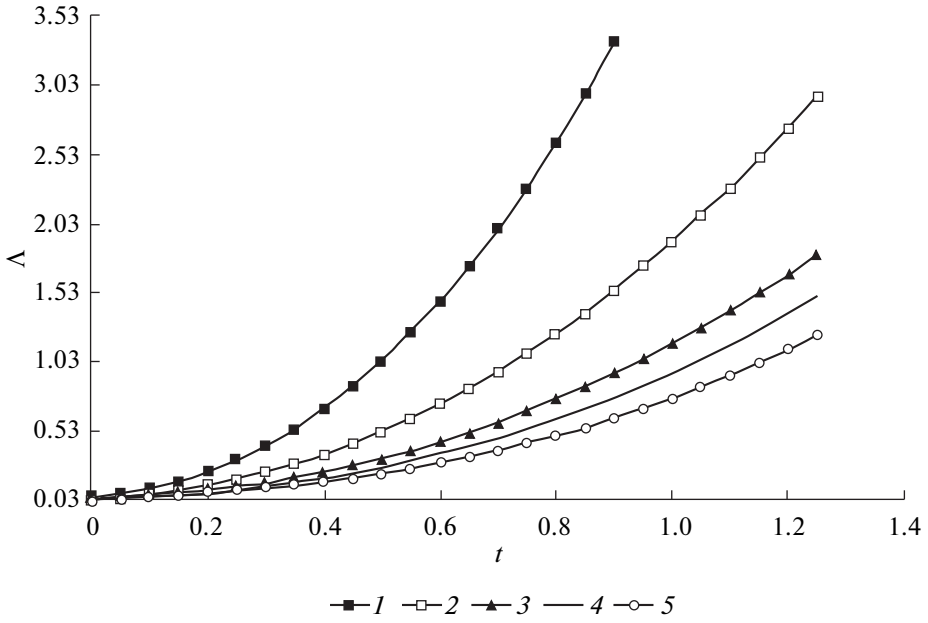

Fig. 2. Change in the integral scale of turbulence calculated at different Reynolds numbers: (1) Re = 5000; (2) Re = 10000; (3) Re = 20000; (4) Re = 30000; (5) Re=50000.

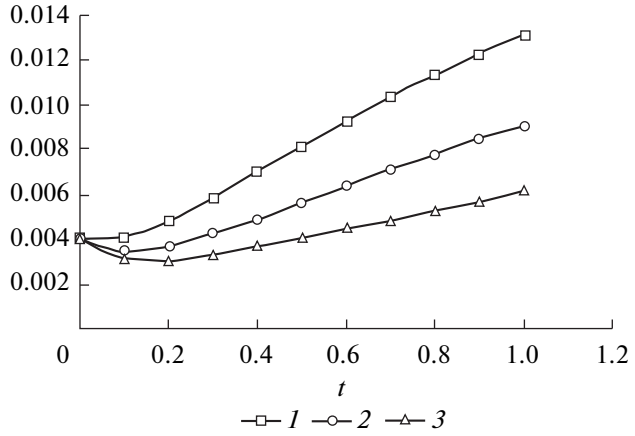

Fig. 3. Change in the micro scale: λ^2 calculated at different Reynolds numbers: (*1*) Re = 5000; (*2*) Re = 10000; (*3*) Re = 20000.

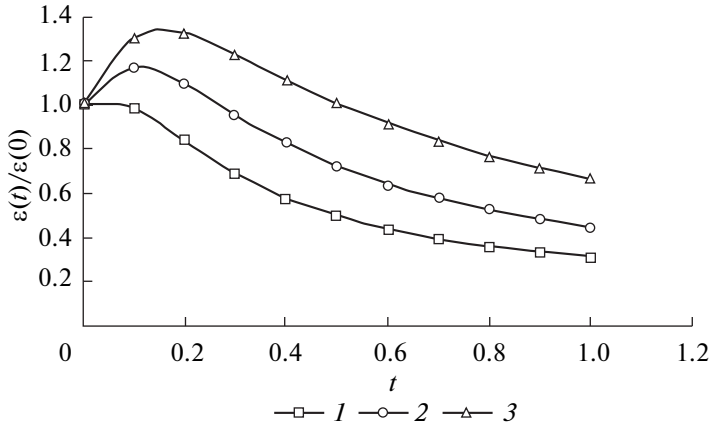

Fig. 4. Change in the energy dissipations calculated at different Reynolds numbers: (*1*) Re = 5000; (*2*) Re = 10000; (*3*) Re = 20000.

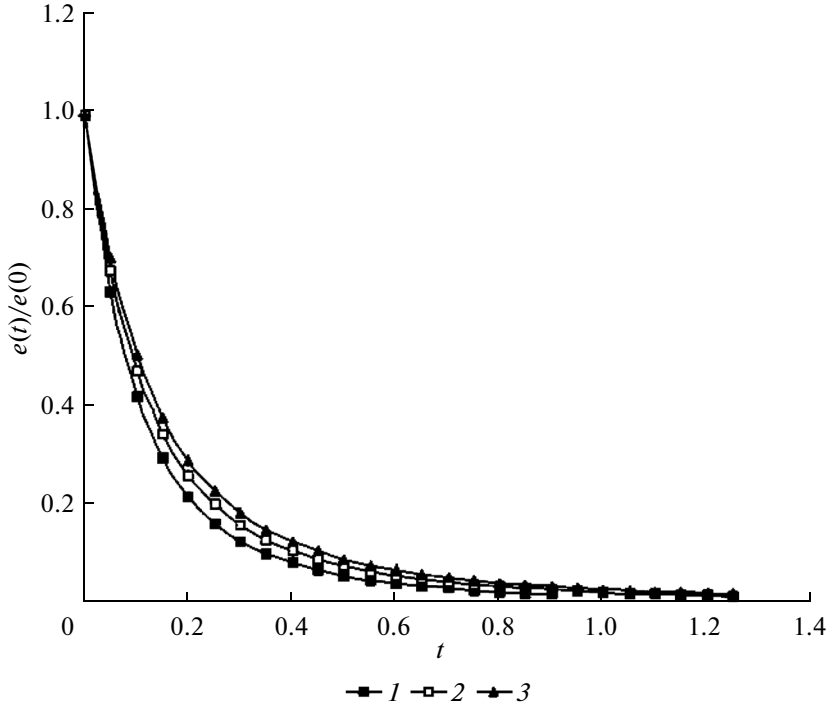

Fig. 5. Temporal variations in the turbulent kinetic energy calculated at different Reynolds numbers: (*1*) Re = 5000; (*2*) Re = 10000; (*3*) Re = 20000.

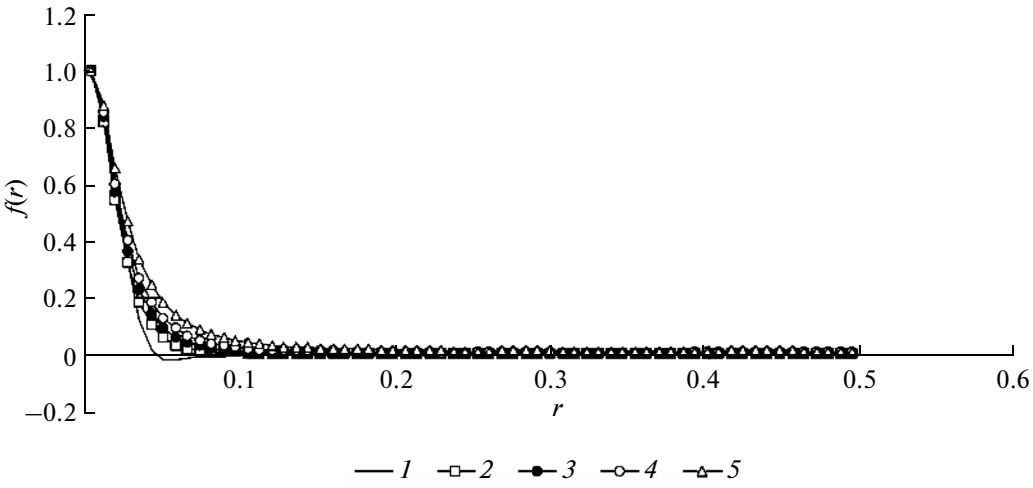

Fig. 6. Temporal variations in the longitudinal correlation function $f(r)$ at Re = 20000: (1) $t = 0$; (2) $t = 0.2$; (3) $t = 0.4$; (4) $t = 0.6$ (5) $t = 1$.

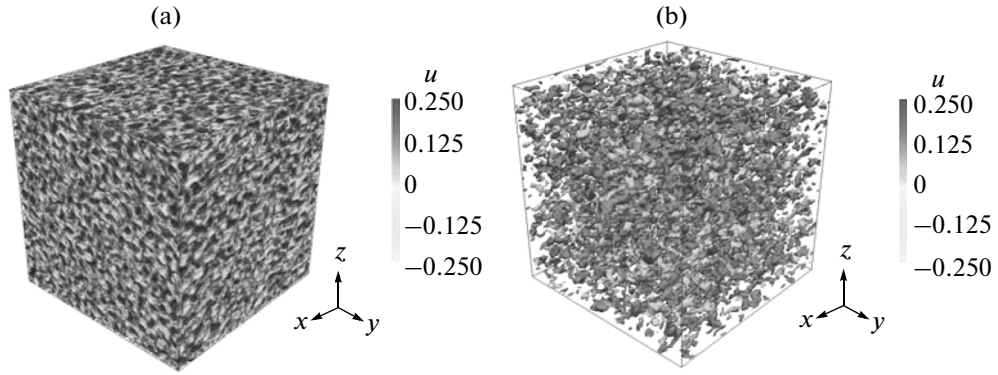

Fig. 7. Component of the velocity u at different timeinstants: (a) $t = 0$; (b) $t = 0.6$.

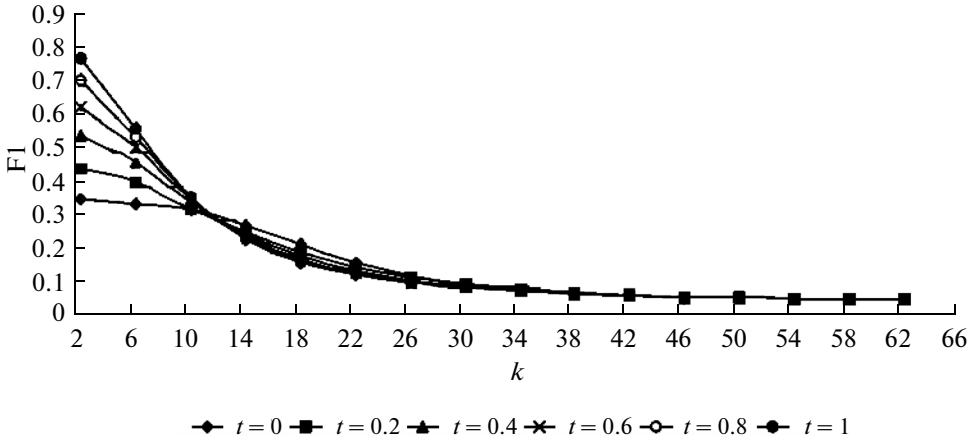

Fig. 8. Change in the longitudinal one-dimensional spectrum calculated at Re = 5000.

Figure 7 presents the velocity component u in the physical space at $t = 0$ and $t = 0.6$. Changes in the one-dimensional longitudinal and transverse spectra at different time moments can be seen in Figs. 8 and 9, respectively, and the three-dimensional spectrum is given in Fig. 10. The values of one-dimensional spectra change monotonically and they are nonnegative; thus, they conform to the requirements of the Khinchin theorem.

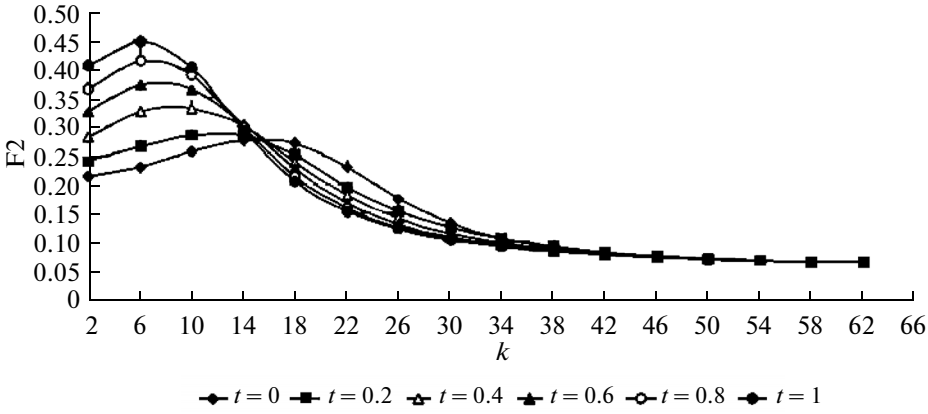

Fig. 9. Change in the transverse one-dimensional spectrum calculated at Re = 5000.

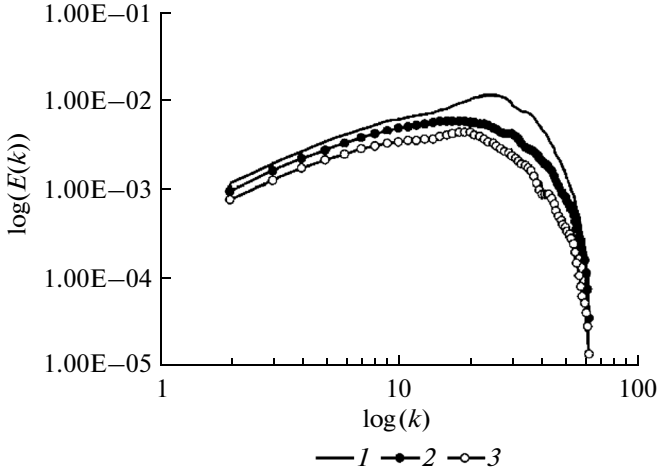

Fig. 10. Change of the three-dimensional spectrum calculated at Re = 10000 and its temporal variation: (1) $t = 0$; (2) $t = 0.4$; (3) $t = 0.8$.

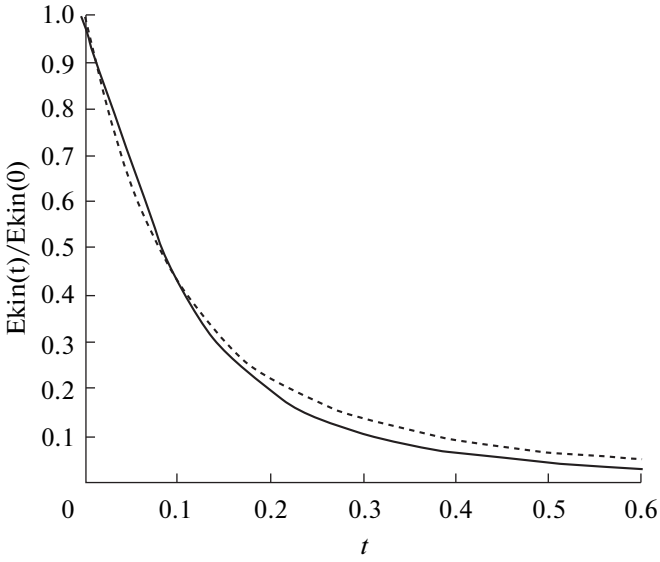

Fig. 11. Change of turbulent kinetic energy in time: the dotted line presents the result of this work; the solid line shows the DNS calculation results [17].

Figure 11 presents the comparison of the results of the temporal degeneration computation of the turbulent kinetic energy obtained in this work with the numerical results of [17] obtained on the basis of the DNS method at $\mathrm{Re}_\lambda = 72$. From the figures it is apparent that the calculation data obtained by the DNS and LES methods are in satisfactory agreement.

6. CONCLUSIONS

Based on the large-eddy method, the numerical simulation of the effect of viscosity on the degeneration of isotropic turbulence is performed.

The analysis of the simulation results enables us to draw the following conclusion. The one-dimensional spectra of the fields have turned out to be nonnegative and monotonic, which corresponds to the requirements of the Khinchin theorem. The flow viscosity significantly affects the turbulence and, therefore, can be used to control it. The results allow a fairly accurate estimation of the time variation in the characteristics of isotropic turbulence at higher Reynolds numbers. In order to find the turbulence spectrum, there is no need to solve the spectral equations, for which it is rather difficult to reach closure.

The results of the numerical simulation obtained in this work are in satisfactory agreement with the findings of other authors [17–19].

Thus, a numerical algorithm for solving the nonstationary three-dimensional Navier–Stokes equations for the simulation of the degeneration of isotropic turbulence at different Reynolds numbers has been developed. The Navier–Stokes equation describes the entire spectrum of problems of the homogenous turbulence. All physical processes and phenomena of homogenous turbulence are discovered in the course of numerical simulation. The method proposed here can be used to solve nonisotropic turbulence without the need for considerable changes.

REFERENCES

1. A. S. Monin and A. M. Yaglom, *Statistical hydromechanics* (Nauka, Moscow, 1967), Chap. 2 [in Russian].
2. J. O. Hinze, *Turbulence: an introduction to its mechanism and theory* (McGraw-Hill, New York, 1959).
3. J. H. Ferziger, "Large Eddy Simulation of Turbulent Flows," AIAA J. **15** (9), 1261–1267 (1977).
4. P. Sagaut, *Large eddy simulation for incompressible flows* (Springer-Verlag Heidelberg, 2002).
5. L. Sirovich, L. Smith, and V. Yakhot, "Energy spectrum of homogeneous and isotropic turbulence in far dissipation range," Phys. Rev. Lett. **72** (3), 344–347 (1994).
6. A. I. Tolstykh, *Compact finite difference schemes and their application to problems in aerodynamics* (Nauka, Moscow, 1990) [in Russian].
7. N. N. Yanenko, *Method of fractional steps for the solution of multidimensional problems in mathematical physics* (Nauka, Novosibirsk, 1967.
8. P. J. Roache, *Computational fluid dynamics* (Hermosa, Albuquerque, NM, 1976).
9. U. S. Abdibekov, B. T. Zhumagulov, and B. D. Surapbergenov, "Numerical simulation of turbulent flows using large-eddy method," Vychisl. Technol. **12** (4) (2007).
10. N. T. Danaev, D. B. Zhakebaev, and A. U. Abdibekov, "Algorithm for solving nonstationary three-dimensional Navier–Stokes equations with large Reynolds numbers on multiprocessor systems," Notes Numer. Fluid Mech. Multidiscip. Des. **115**, 313–326 (2011).
11. U. S. Abdibekov, B. T. Zhumagulov, and D. B. Zhakebaev, "Numerical modeling of non-homogeneous turbulence on cluster computing system," Notes Numer. Fluid Mech. Multidiscip. Des. **115**, 327–338 (2011).
12. V. M. Ievlev, *Numerical simulation of turbulent flows* (Nauka, Moscow, 1990) [in Russian].
13. H. Tennekes and J. L. Lumley, *A first course in turbulence* (MIT Press, Cambridge, MA, 1972)
14. S. A. Orszag and G. S. Patterson, "Numerical simulation of three-dimensional homogeneous isotropic turbulence," Phys. Rev. Lett. **28** (2), 76–79 (1972).
15. A. M. Obukhov and A. M. Yaglom, Microstructure of a turbulent flow, Prikl. Mat. Mekh, No. 13, 3–26 (1951).
16. N. de Divitiis, "Lyapunov analysis for fully developed homogeneous isotropic turbulence," Theor. Comput. Fluid Dyn. **25** (6), 421–445 (2011)
17. D. E. Goldstein, O. V. Vasilyev, and N. K. Kevlahan, "CVS and SCALES simulation of 3-D isotropic turbulence," J. Turb. **6** (37), 1–20 (2005).
18. G. De Stefano, D. E. Goldstein, and O. V. Vasilyev, "On the role of sub-grid scale coherent modes in large eddy simulation," J. Fluid Mech. **525**, 263–274 (2005).
19. K. Schneider and O. V. Vasilyev, "Wavelet methods in computational fluid dynamics," Ann. Rev. Fluid Mech. **42**, 473–503 (2010).

Translated by I. Pertsovskaya

SPELL: 1. nonstationary